16th World Conference on Earthquake, 16WCEE 2017

Santiago Chile, January 9th to 13th 2017

Paper N° 1236

Registration Code: S-B1464580037

BRITTLE COMPRESSION FAILURES IN ACI 318-14 COMPLIANT RC STRUCTURAL WALLS WITH WELL-DETAILED BOUNDARY ZONES

C.L. Segura [1] and J.W. Wallace [2]

[1] *PhD Student, Department of Civil and Environmental Engineering, University of California, Los Angeles, segurac@ucla.edu*
[2] *Professor, Department of Civil and Environmental Engineering, University of California, Los Angeles, wallacej@ucla.edu*

Abstract

Field observations following recent earthquakes (2010 Chile, 2011 New Zealand) identified the vulnerability of flexure-dominant shear walls to brittle compression and strength loss, apparently prior to developing significant inelastic deformation capacities. To better understand the performance limitations of modern, code-compliant shear walls, two shear wall panels were tested under combined axial load and increasing cyclic moment and shear. The wall panel specimens represented the lower portion of a cantilever wall within an 8-story building. One wall had a rectangular cross-section, and the other had a T-shape cross-section with an enlarged boundary at one end of the wall. Test variables included the arrangement of boundary longitudinal and transverse reinforcement, and depth of the compression zone (influenced by axial load and quantity of longitudinal reinforcement). For both tests, axial load was held constant ($P_u/A_w f'_c$=0.10). Brittle compression failures were observed for both walls at plastic rotations, measured over an assumed plastic hinge length of one-half the length of the wall, between 0.01 and 0.015 radian. Test results indicate that brittle failures occurred because of the inability of thin compression zones to distribute compression strains over a significant height following crushing/spalling of unconfined concrete at wall edges.

Keywords: reinforced concrete; structural wall; detailing

1. Introduction

The use of reinforced concrete structural walls (shear walls) as the primary lateral force-resisting system in buildings is widespread due to their stiffness and strength, ductility, and energy dissipating capabilities. Field observations of shear walls following earthquakes in Chile and New Zealand reported damage indicative of brittle compression failures for walls designed according to modern codes [1, 2, 3]. Observed damage included crushing of wall boundary regions, buckling of longitudinal reinforcement, fracture/pullout of boundary transverse reinforcement, and out-of-plane instability of compression zones. Lack of well-confined boundary regions are suspected to have contributed to poor performance [4, 5]; however, brittle compression failure modes have been observed in recent laboratory tests on code-compliant walls with well-confined boundaries [6, 7], and the mechanisms leading to the failures are not yet well understood.

An experimental program was conducted at the University of California, Los Angeles to assess the deformation capacity and failure modes of thin, code-compliant walls. Two wall panel specimens, representing the lower portion of a cantilever wall, were tested under combined axial load and increasing cyclic moment and shear. Both walls satisfied ACI 318-14 Special Structural Wall provisions. ACI 318-14 allows the use of a displacement-based design approach to determine the need for Special Boundary Element (SBE) detailing [8]. SBE detailing is required when:

$$c \geq \frac{l_w}{600(1.5)(\delta_u / \mathrm{h}_w)} \tag{1}$$

where c is the largest neutral axis depth determined for the factored axial load and nominal flexural capacity consistent with the design roof displacement δ_u, l_w is the length of the wall, and h_w is the height of the wall. Design roof drift (δ_u,/h_w) is not to be taken smaller than 0.005 in Eqn. 1. Fig. 1 demonstrates the impact of compression depth on the need for SBE detailing for roof drift demands up to 0.02.

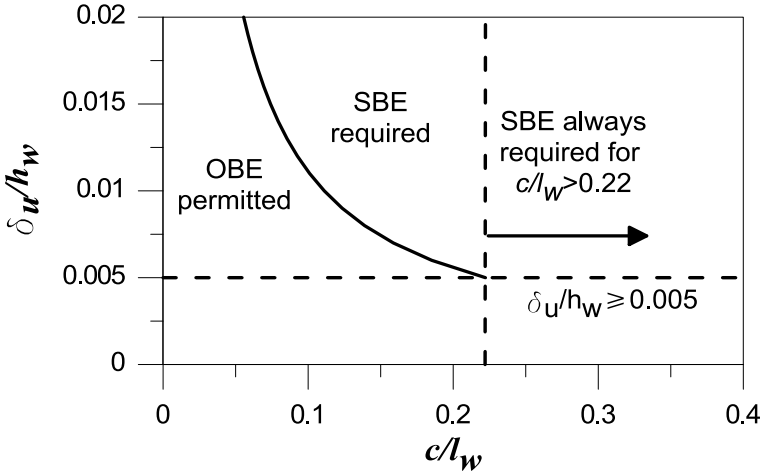

Fig. 1 – Impact of compression depth (c/l_w) and roof drift (δ_u/h_w) on the need fro SBE detailing

Where SBE detailing is required, boundary transverse reinforcement must satisfy Eqn. 2a and Eqn. 2b:

$$\frac{A_{sh}}{sb_c} \geq 0.09 \frac{f'_c}{f_{yt}} \tag{2a}$$

$$\frac{A_{sh}}{sb_c} \geq 0.3 \left(\frac{A_g}{A_{ch}} - 1 \right) \frac{f'_c}{f_{yt}} \tag{2b}$$

where s is the vertical spacing of boundary transverse reinforcement, b_c is the cross-sectional dimension of the core measured to the outside edges of transverse reinforcement, A_{sh} is the quantity of transverse reinforcement provided within spacing s and perpendicular to b_c, A_g is the gross area of the confined section, A_{ch} is the area of

the core section measured to the outside of hoops, f'_c is the specified concrete compressive strength, and f_{yt} is the specified yield strength of the transverse reinforcement.

Where SBE detailing is not required, vertical spacing of transverse reinforcement (s) is limited to the minimum of 200mm and eight times the longitudinal bar diameter (d_d), except in yielding regions, where s is limited to 150mm or $6d_b$.

2. Experimental Program

Two approximately one-half scale wall panel specimens were tested in the University of California, Los Angeles Structural/Earthquake Engineering Laboratory (SEERL). The test specimens represented the lower portion of an eight story cantilever wall. Design concrete compressive strength (f'_c) and reinforcing steel yield strength (f_y) were 34.5MPa and 414MPa, respectively. The walls were designed for an axial load demand (P_u) of $0.10A_w f'_c$, where A_w is the area of the wall web.

2.1 Test Setup and Instrumentation

The test setup is shown in Fig. 2. The walls were tested in an upright position. Test specimens were cast monolithically with a thickened footing and top cap beam. Axial load was held constant throughout the tests using two hydraulic jacks attached to high-strength post-tensioning bars anchored to the laboratory strong floor. Increasing cyclic moment and shear was applied using two vertical actuators and one horizontal actuator. The shear span (M/V) was held constant throughout the tests to achieve the bending moment gradient expected in the lower portion of a cantilever wall. An out-of-plane support system was attached to a strong wall parallel to the specimens to prevent out-of-plane movement of the specimen top cap beams.

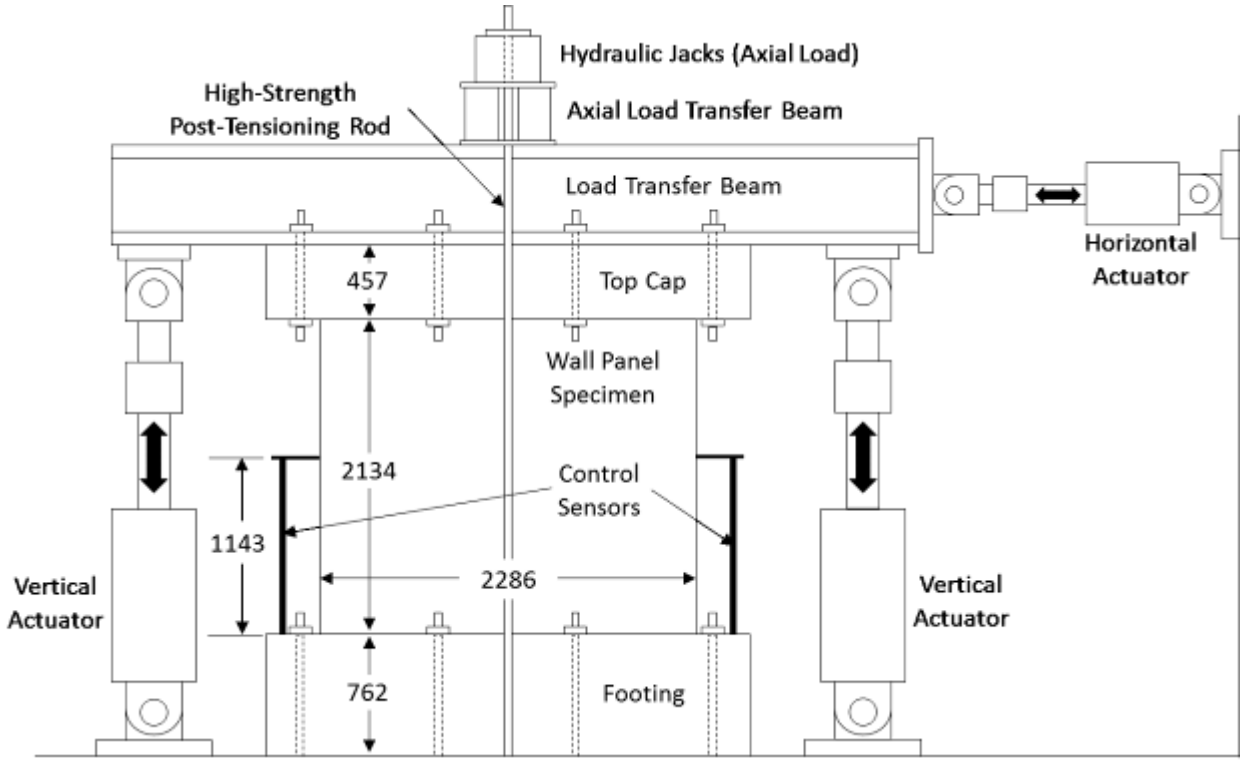

Fig. 2 – Test Setup (dimensions in mm)

For each wall, approximately forty strain gages were used to measure reinforcing bar strains at various locations. Approximately fifty-five linear variable differential transducers (LVDTs) were mounted to the front and rear faces of the specimens (Fig. 3). Columns of vertically-mounted LVDTs were used to measure wall

flexural deformations over the height of the specimens. Wall shear deformations were measured using three pairs of LVDTs arranged in X-configurations. Wall lateral drift was measured using three horizontally-mounted LVDTs attached to a rigid reference frame. Top cap beam out-of-plane deformations were measured at each end of the top caps using horizontally-mounted LVDTs attached to a strong wall parallel to the test specimens. Average rotation was measured between two vertically-mounted LVDTs positioned at opposite ends of the wall.

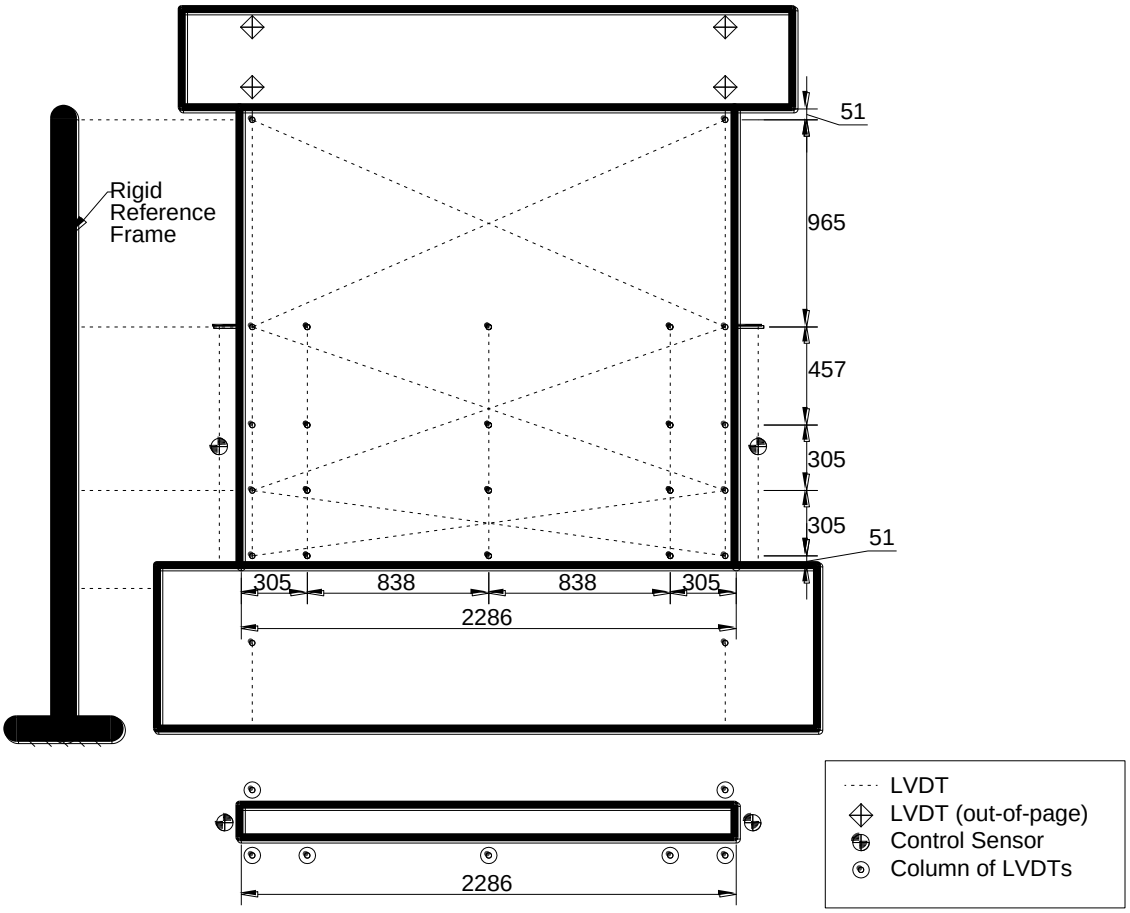

Fig. 3 – Instrumentation (dimensions in mm)

2.1 Specimen Details

The experimental testing matrix is shown in Table 1. The primary variables were the arrangement of longitudinal reinforcement (WP2) and compression depth (WP4). Boundary transverse reinforcement was selected to satisfy ACI 318-14 minimum requirements for Special Structural Walls (ACI 318 designation).

Table 1 – Specimen testing matrix

Test Specimen	**s/d_b** ---	**c/L_w** ---	**$A_{sh,y}/sb_{c,y}$** [%]	**$A_{sh,x}/sb_{c,x}$** [%]	**$A_{sh,req}/sb_c$**		**$A_{sh}/A_{sh,req}$** ---
					Eq. 2a [%]	**Eq. 2b** [%]	
WP2	3.20	0.20	1.28	1.78	1.23	0.75	1.04
	4.00						
WP4 (web)	3.20	0.30	1.21	1.78	1.14	0.75	1.07

Cross-sectional geometries and reinforcement are shown in Fig. 4. Both test specimens were 2134mm in height, 2286mm in length, and 152mm thick. Boundary longitudinal reinforcement for WP2 consisted of eight 15.9mm diameter bars at the west boundary (ρ_{lb}=2.92%) and fourteen 12.7mm diameters bars at the east boundary (ρ_{lb}=3.27%). Web longitudinal and transverse reinforcement consisted of 9.5mm diameter bars spaced at 203mm on-center (ρ_{lw} =ρ_{lv}=0.46%). Web longitudinal bars were placed outside of web transverse bars (Fig. 4a) as allowed by ACI 318-14. Compression depth, determined using an extreme fiber compression strain of 0.003 (consistent with ACI 318-14 requirement) for an axial load of $0.10A_w f'_c$, was $0.21l_w$ and $0.20l_w$ for loading causing compression at the west boundary and east boundary, respectively. For typical design roof drift demands (e.g., δ_u/h_w=0.01-0.02), SBEs are required at both wall boundaries (Fig. 1). SBE detailing at each boundary consisted of an 8.1mm diameter hoop and two cross-ties spaced at 51mm on-center (s/d_b=*3.2* and *4.0* at west and east boundaries, respectively). Boundary transverse reinforcement ratio (A_{sh}/sb_c) was 1.28%.

Specimen WP4 was constructed with an enlarged boundary region (flange) at the east end of the wall (Fig. 4b). The flange accommodated more longitudinal reinforcement at the east boundary, making it possible to impose a longer compression depth at the web boundary as would be expected for a wall with higher axial load demand (e.g., $0.20A_w f'_c$) or a wall with an asymmetric cross-section (e.g. T-shape wall). Boundary longitudinal reinforcement for WP4 consisted of ten 15.9mm diameter bars at the west (web) boundary (ρ_{lb}=2.84%) and fourteen 19.1mm diameters bars at the east (flange) boundary. Web longitudinal and transverse reinforcement was identical to that of specimen WP2. Compression depth, determined using an extreme fiber compression strain of 0.003 for an axial load of $0.10A_w f'_c$, was $0.30l_w$ and $0.06l_w$ for loading causing compression at the web and flange boundaries, respectively. For typical roof drift demands, SBE detailing is required at the web boundary only (Fig. 1). SBE detailing at the web boundary consisted of an 8.1mm diameter hoop and three cross-ties spaced at 51mm on-center (s/d_b=*3.2*, A_{sh}/sb_c=1.21%). OBE detailing at the flange boundary consisted of two overlapping 6.4mm diameter hoops spaced at 114mm on-center (s/d_b=*6.0*).

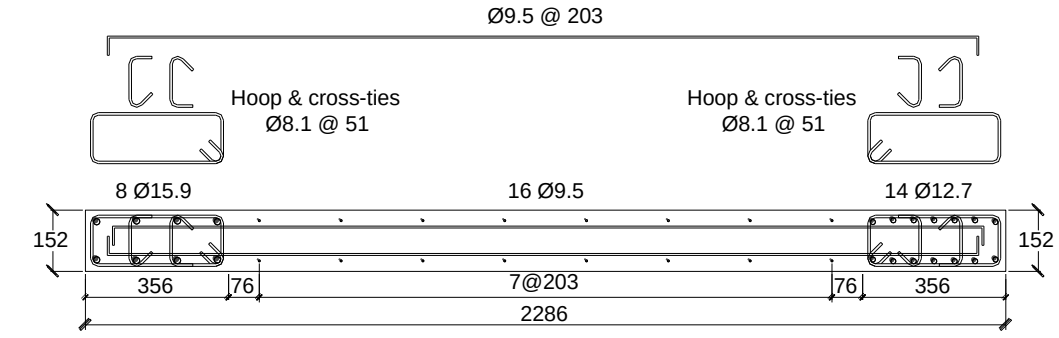

a)

b)

Fig. 4 – Specimen cross-sections: a) WP2; and b) WP4

2.2 Experimental Results

Normalized base overturning moment vs. hinge rotation results are shown in Fig. 5. Hinge rotation was measured by two control sensors, positioned at opposite ends of the wall, over an assumed hinge length of one-half the length of the wall (Fig. 3). For each plot, the ASCE 41 modeling backbone is included [9].

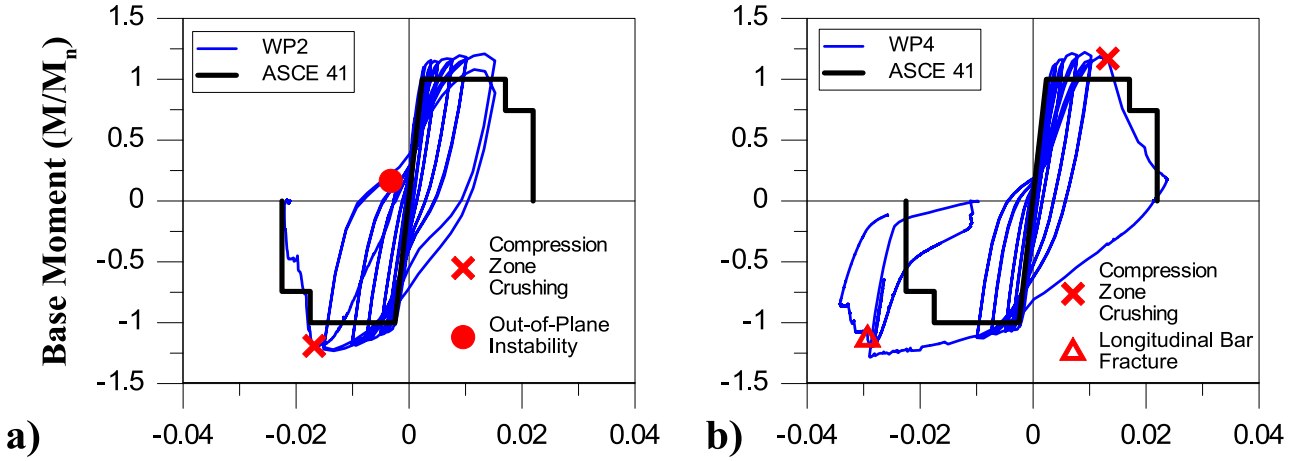

Fig. 5 – Experimentally Measured Base Overturning Moment vs. Hinge Rotation

For specimen WP2, crushing of cover concrete at both ends of the wall was observed during the first 1.5% hinge rotation loading cycle. Minor crushing at the west boundary was observed during the next loading cycle, resulting in a reduction in strength of approximately 30%. Lateral instability at the west boundary was observed while attempting a third loading cycle to +1.5% hinge rotation. The instability occurred at a small positive load, and little residual strength remained for loading in the positive direction. Monotonic loading was applied in the negative direction until failure. At approximately -1.7% hinge rotation, abrupt crushing at the east boundary occurred (Fig. 6a). Crushing of concrete extended approximately one-third the length of the wall from the east boundary, and damage was concentrated within the bottom 350mm above the base of the wall. Buckling of all boundary longitudinal reinforcement and the four web longitudinal bars closest to the east boundary was observed (Fig. 6b). Two fractured boundary hoops were removed from the specimen, and pullout/opening of several 90-degree cross-tie hooks was observed in the damaged region (Fig. 6c). It is noted that initial opening of 90 degree cross-tie hooks was observed following spalling of cover concrete in previous cycles. At the instant failure occurred, axial load capacity dropped approximately 20% from $0.10A_w f'_c$ to $0.08A_w f'_c$, and very little residual strength remained. The specimen was unable to achieve 2% plastic rotation capacity at a residual strength of 75% of the nominal flexural strength, as assumed by ASCE 41.

For specimen WP4, crushing occurred at the web boundary at approximately +1.3% hinge rotation (Fig. 7a) with no prior sign of strength loss. Damage concentrated within the bottom 350mm of the wall, and extended horizontally approximately two-thirds the length of the wall. Out-of-plane displacement of the compression zone occurred near the base of the wall, in the damaged region (Fig. 7b). A maximum out-of-plane displacement of 60mm was measured approximately 300mm above the base of the wall. Removal of lose concrete revealed buckling of several boundary longitudinal bars and a few web longitudinal bars, fracture of boundary hoops, and failure of 90 degree cross-tie hooks. A 60% reduction in axial capacity occurred as axial load instantaneously dropped to approximately $0.04A_w f'_c$. Like specimen WP2, WP4 was unable to achieve the deformation capacity and residual strength assumed by ASCE 41.

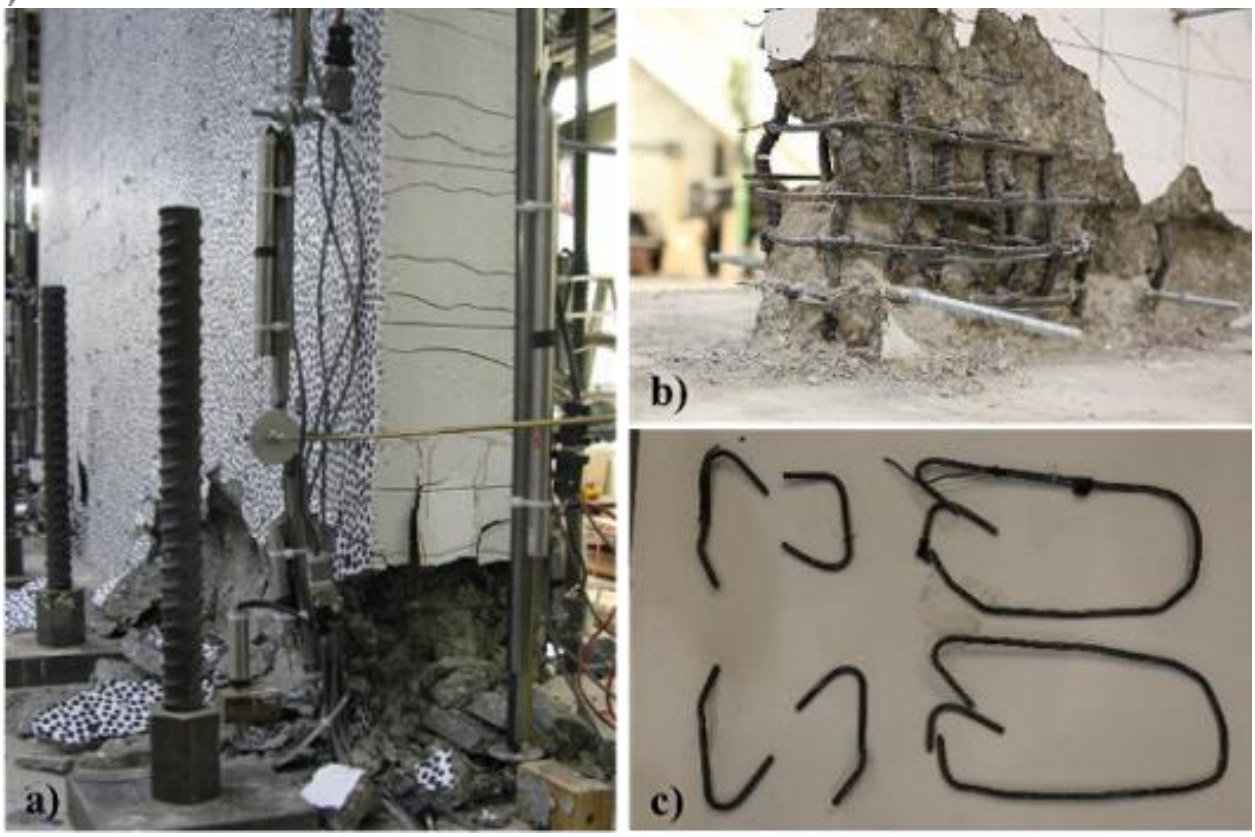

Fig. 6 – WP2: a) Damage at east edge; b) Buckled reinforcement; and c) Transverse reinforcement

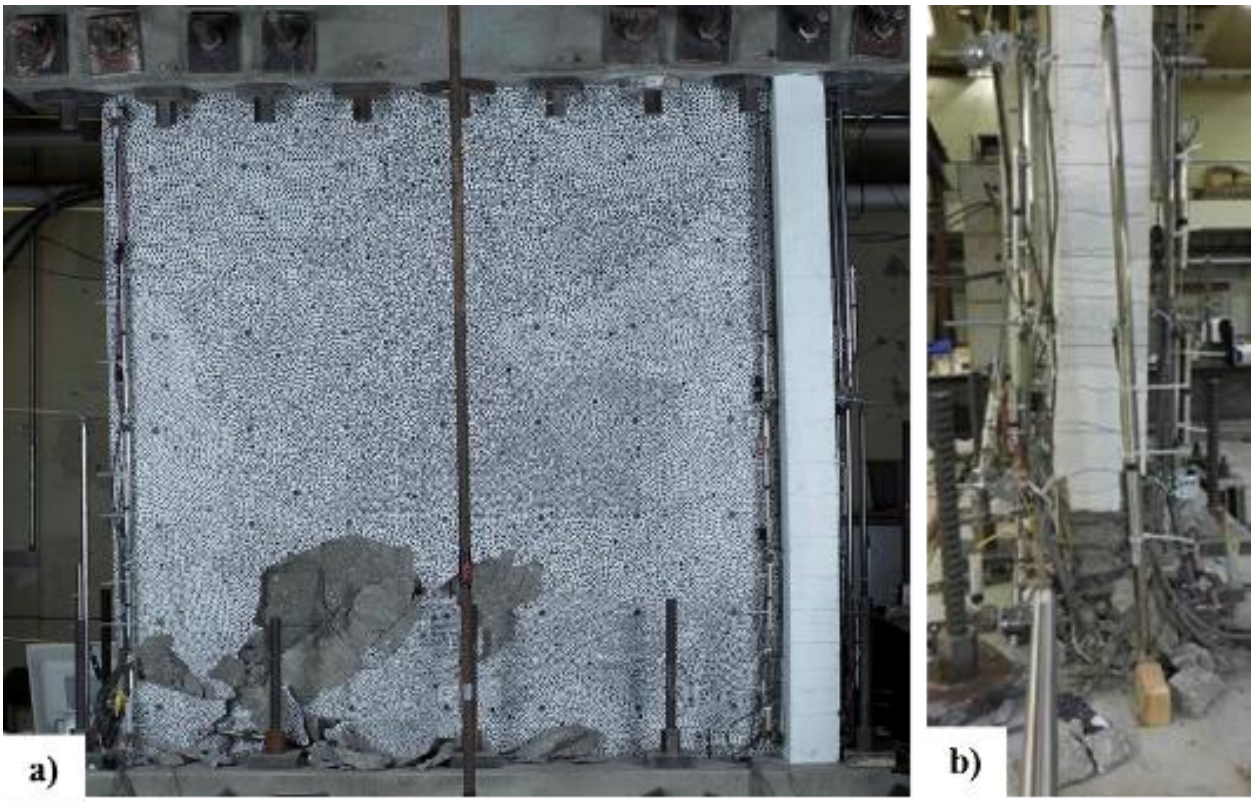

Fig. 7 – WP4: a) Boundary and web crushing; and b) Out-of-plane displacement

Backbone curves of the average extreme fiber compression strain, measured by sensors at three different heights, are presented in Fig. 8a for specimen WP4. On each plot, the average strain measured over a gage length of one-half the length of the wall ($L_w/2$) is plotted as a light gray line. From the figure, it can be seen that compression strains concentrate over a short height (Lev 1 in Fig. 8a). Concentration of strains occurs following minor crushing/spalling of unconfined concrete at the edge of the wall, leading to large strain demands in the critical section (Lev 1). Just before strength loss, the measured compression strain at Lev 1 was approximately 0.025, while the sections above remained elastic. Similar results were obtained for specimen WP2. In Fig. 8b, a comparison of the Lev 1 extreme fiber compression strain backbones is made for specimen WP2 and WP4. Lev 1 strains were measured over a gage length of 350mm, approximately the height of the damaged region in both tests. A circular marker indicates the point at which failure initiated in each test. At the onset of failure, the Lev 1 compression strain for specimens WP2 and WP4 were 0.0284 and 0.0228, respectively. At the same instant, average compression strains, over gage length $L_w/2$, of 0.0093 and 0.0080 were measured for WP2 and WP4, respectively.

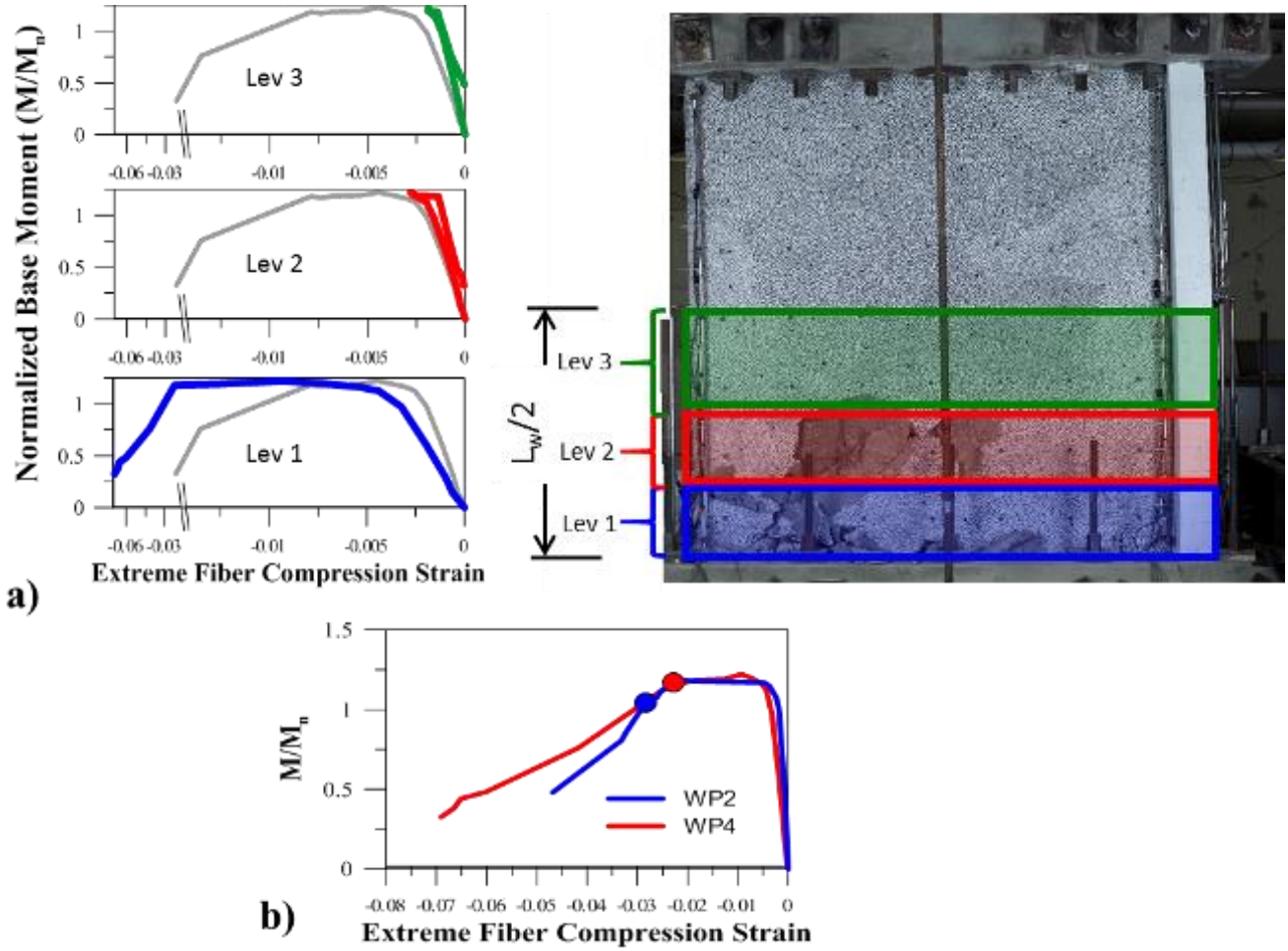

Fig. 8 – Extreme fiber compression strains a) WP4 at different heights; and b) WP2 and WP4 (Lev 1)

3. Conclusions

Experimental results were presented for two shear wall panel specimens designed with boundary transverse reinforcement satisfying ACI 318-14 provisions for Special Structural Walls. Brittle compression failures were observed at wall boundaries in both tests at plastic rotations, measured over an assumed hinge length of one-half the length of the wall ($L_w/2$), of approximately 1.5% and 1.0% for specimen WP2 and specimen WP4, respectively. For both walls, measured rotation capacity and residual strength were less than the values assumed

by ASCE 41. Sensors positioned at wall edges indicated that compression strains concentrated over a short height approximately equal to two-and-a-half times the thickness of the wall. Average extreme fiber compression strains, measured over a gage length of $L_w/2$, were less than 0.01 at the onset of failure.

Ongoing research is being conducted to define reliable drift and strain limits to avoid the brittle failure modes observed in these tests. Furthermore, the performance of walls with thicker cross-sections and/or overlapping boundary transverse hoops is being investigated to understand the role of wall geometry and boundary detailing on the compression strain capacity and drift capacity of walls.

4. Acknowledgements

Experimental testing was conducted in the University of California, Los Angeles Structural/Earthquake Engineering Laboratory with funding provided by the National Science Foundation (NSF) Grant CMMI 1208192. The laboratory was renovated with funds provided by the NSF under grant No. 0963182, an award funded under the American Recover and Reinvestment Act of 2009. Any opinions, findings, and conclusions or recommendations expressed in this material are those of the authors and do not necessarily reflect the views of the NSF.

5. References

[1] Alarcón, C., Hube, M.A., Jünemann, R., & de la Llera, J.C. (2015). Characteristics and displacement capacity of reinforced concrete walls in damaged buildings during 2010 Chile earthquake, *Bulletin of Earthquake Engineering*, Vol 13(4), 1119-1139.

[2] Wallace, J. W., Massone, L. M., Bonelli, P., Dragovich, J., Lagos, R., Luders, C., & Moehle, J. P. (2012). Damage and implications for seismic design of RC structural wall buildings, *Earthquake Spectra*, Vol 28(S1), S281-S299.

[3] Kam, W.Y., Pampanin, S., & Elwood, K. (2011). Performance of concrete buildings in the 22 February Christchurch (Lyttelton) earthquake, *Bulletin of the New Zealand Society for Earthquake Engineering*, 44(4), 239-278.

[4] Wallace, J. W. (2012). Behavior, design, and modeling of structural walls and coupling beams – Lessons from recent laboratory tests and earthquakes, *International Journal of Concrete Structures and Materials*, Vol 6(1), 3-18.

[5] Massone, L. M., Bonelli, P., Lagos, R., Luders, C., Moehle, J. P., & Wallace, J. W. (2012). Seismic design and construction practices for RC structural wall buildings, *Earthquake Spectra*, Vol 28(S1), S245-S256.

[6] Lowes, L.N., Lehman, D.E., Birely, A.C., Kuchma, D.A., Marley, K.P., & Hart, C.R. (2012). Earthquake response of slender planar concrete walls with modern detailing, *Engineering Structures*, Vol 43, 31-47.

[7] Nagae, T., Tahara, K., Fukuyama, K., Matsumori, T., Shiohara, H., Kabeyasawa, T., Kono, S., Nishiyama, M., Moehle, J., Wallace, J., Sause, R., Ghannoum, W. (2012). Test results of four-story reinforced concrete and post-tensioned concrete buildings: The 2010 E-Defense shaking table test, *Proceedings of the Fifteenth World Conference on Earthquake Engineering (15WCEE)*, Lisbon, Portugal.

[8] ACI Committee 318 (2014). Building Code Requirements for Structural Concrete and Commentary (ACI 318-14). Farmington Hills, MI: American Concrete Institute.

[9] ASCE/SEI (2013). Seismic Rehabilitation and Upgrade of Existing Buildings (ASCE/SEI 41-13). American Society of Civil Engineers, Reston, Virginia.